Erosion of a 1,3-Bis(*p*-carboxyphenoxy)propane−Sebacic Acid Poly(anhydride) Copolymer by Water Vapor Studied by ^{1}H and ^{13}C Solid-State NMR Spectroscopy

Frank Heatley,*,† Mohammad Humadi,† Robert V. Law,†,‡ and Antony D'Emanuele§

Department of Chemistry and School of Pharmacy and Pharmaceutical Sciences, University of Manchester, Manchester M13 9PL, U.K.

Received November 10, 1997; Revised Manuscript Received March 25, 1998

ABSTRACT: The erosion of a 1,3-bis(*p*-carboxyphenoxy)propane−sebacic acid poly(anhydride) copolymer, p(CPP:SA), by water vapor has been studied by ^{1}H wide-line and ^{13}C MAS solid-state NMR spectroscopy. In contrast to erosion by phosphate buffer, no mobile absorbed water was detected. ^{1}H T_1, $T_{1\rho}$, and line width data indicated that the polymer matrix became more rigid on erosion due to the formation of crystalline degradation products. From the ^{13}C spectra, the hydrolysis of the anhydride links into SA and CPP carboxylic acid groups was determined quantitatively. The rate of hydrolysis by water vapor was comparable to that by phosphate buffer. The SA−SA and SA−CPP links were hydrolyzed at comparable rates, and both were hydrolyzed more rapidly than CPP−CPP links.

Introduction

Copolyanhydrides of 1,3-bis(*p*-carboxyphenoxy)propane (CPP) and sebacic acid (SA), p(CPP:SA) (Chart 1), have been extensively used as biodegradable carriers for drug delivery applications. It is important to characterize the rates and extents of physicochemical changes occurring within polymer matrixes during erosion. The morphological characterization of polyanhydrides has been carried out using scanning electron microscopy,[1] light microscopy,[2] and most recently in situ atomic force microscopy[3] and magnetic resonance imaging.[4,5] Göpferich and Langer have examined the influence of polymer microstructure and monomer solubility on the erosion process,[6] and Göpferich has proposed a model to predict porosity and mass balance changes occurring within eroding matrixes.[7] The sequence structure of p(CPP:SA) has been characterized by liquid-state ^{1}H NMR[8] and by FTIR.[9] We have recently reported an investigation into the erosion by pH 7.4 phosphate buffer of p(CPP:SA) copolymers containing 12.5 and 30 mol % CPP using ^{1}H high-resolution (liquid-state) NMR to monitor changes in the chemical structure, and ^{1}H and ^{2}H wide-line (solid-state) NMR to monitor morphological changes.[10] This work showed that SA−SA and SA−CPP anhydride links were hydrolyzed at approximately the same rate, and both were hydrolyzed much more rapidly than CPP−CPP links. After 48 h at 37 °C, ca. 50% of each of the SA−SA and SA−CPP links were hydrolyzed, the degree of polymerization decreasing from 48.5 to 3. After ca. 12 h, there was a rapid increase in water absorption, amounting to 70−80 wt % after 48 h. Simultaneously, there was an increase in the proportion of immobile protons in the polymer, attributed to the formation of crystalline domains of SA monomer. However, there have been no reports of the use of other widely used solid-state NMR techniques such as ^{1}H relaxation measurements or ^{13}C magic-angle spinning (MAS) to study the solid-state characteristics of copoly(anhydrides). The objective of the present study was to investigate the application of these methods to the chemical and morphological changes occurring during erosion of p(CPP:SA) polyanhydrides. At the same time, the opportunity was taken to study the erosion of p(CPP:SA) exposed to water vapor in order to characterize erosion in materials exposed to atmospheric conditions and to compare the results with those for materials exposed to aqueous buffer. A possibly significant difference between the two media is that in erosion by water vapor, there is no possibility of losing low molecular weight degradation products by solubilization in the aqueous phase.

Experimental Section

Materials. The copolymer studied was a statistical p(CPP:SA) copolymer containing 20 mol % CPP, prepared by melt polycondensation of mixed anhydrides of the diacids and acetic acid, as described previously.[11] To achieve the uniform packing necessary for ^{13}C magic-angle spinning experiments, the polymer was ground into a powder with an average particle size of ca. 0.2 mm. For comparison, spectra were also recorded for the individual CPP and SA diacid monomers.

Degradation Procedure. Before these experiments, the polymer had been stored under nitrogen at −10 °C. The powdered polymer was spread out in a one particle-thick layer in a Petri dish and placed on a grid above liquid water in a closed vessel at room temperature (21 °C) for periods of time up to 104 h. The same sample was used throughout. Care was taken to keep the polymer cold in a dry atmosphere when not exposed to water vapor. There was no evidence of changes in composition while carrying out the lengthy ^{13}C NMR experiments, presumably due to being kept in a tightly sealed rotor in an NMR probe continuously flushed with dry air. To provide a valid comparison, the CPP and SA monomers were exposed to water vapor under the same conditions before running their NMR spectra.

NMR Spectroscopy. NMR spectra were obtained at ambient temperature using a Varian Associates Unity 300 spectrometer operating at 300 MHz for ^{1}H and equipped with probes from Doty Scientific, Inc. Wide-line ^{1}H spectra were obtained using a 5 mm CRAMPS probe without magic-angle spinning (MAS), the polymer powder being packed into short

* To whom correspondence should be addressed.
† Department of Chemistry.
‡ Present address: Department of Chemistry, Imperial College, London SW7 5AY, U.K.
§ School of Pharmacy and Pharmaceutical Sciences.

S0024-9297(97)01652-5 CCC: $15.00
Published on Web 05/15/1998

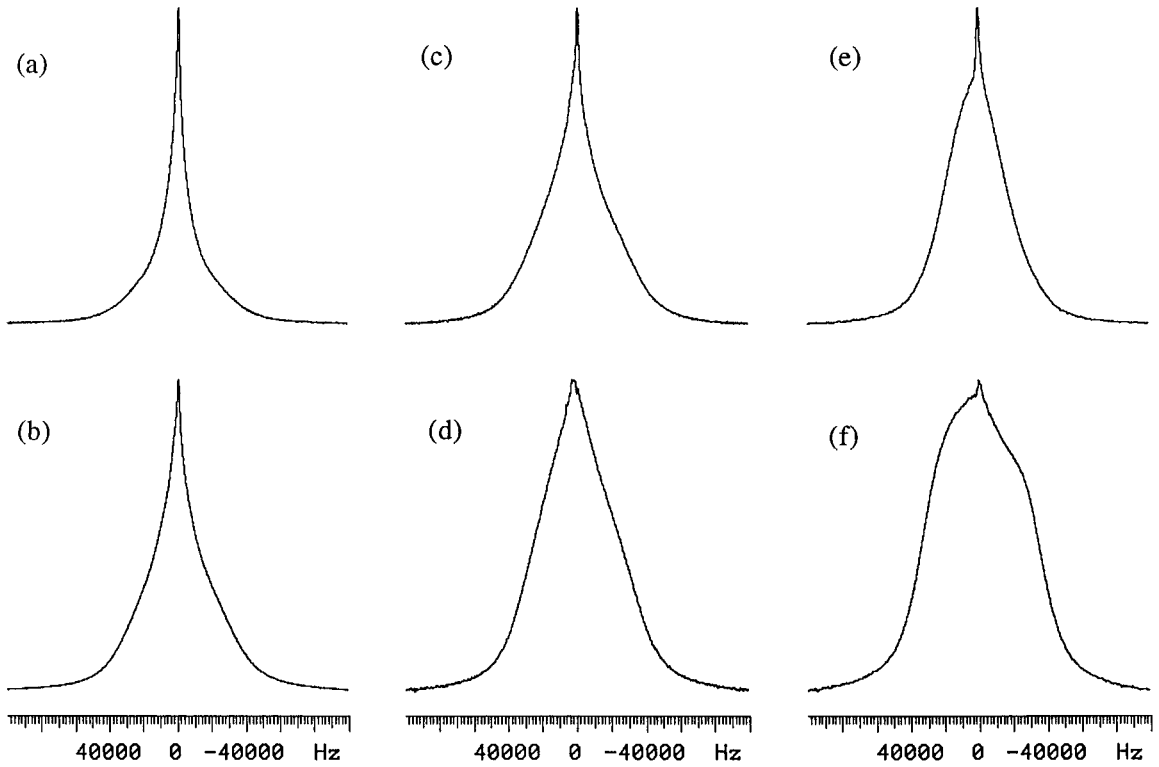

Figure 1. ^{1}H wide-line spectra of p(CPP:SA) 20:80 exposed to water vapor, and of CPP and SA monomers: (a) original copolymer; (b) 3 h of exposure; (c) 18 h of exposure; (d) 104 h of exposure; (e) CPP monomer; (f) SA monomer.

Table 1. Component Analysis of ^{1}H Wide-Line Spectra

exposure time/h	broad		intermediate		narrow	
	line width/kHz	proportion/%	line width/kHz	proportion/%	line width/kHz	proportion/%
0	52	52	13	42	2.4	6
3	53	75	14	22.5	2.6	2.5
10	51	83	10	16	1.5	1
18	53	82	12.5	16	1.8	2
42	54	89	13	11		
104	55	91	13	9		
CPP	41	100				
SA	66	100				

5 mm o.d. Pyrex glass tubes. ^{1}H longitudinal relaxation times (T_{1H}) and rotating-frame relaxation times ($T_{1\rho H}$) were measured by standard techniques.[12] The Goldman−Shen technique[13] was used to investigate spin diffusion. Component analysis of ^{1}H wide-line spectra was carried out using manufacturer-supplied software. ^{13}C MAS spectra were obtained using a 7 mm o.d. MAS probe, the polymer powder being packed into zirconia or alumina rotors with Kel-F end caps. ^{13}C spectra were obtained with high-power ^{1}H decoupling using both cross-polarization (CP) and single-pulse excitation (SPE) methods[14] at a spin rate of ca. 5 kHz. The $\pi/2$ pulse width was 7 μs. In the CP technique, the ^{13}C signal is generated by transfer of nuclear magnetization from protons by spin diffusion under Hartmann−Hahn matched spin locking, and the technique therefore discriminates in favor of relatively rigid species capable of undergoing efficient cross-polarization. The variation of ^{13}C intensity as a function of contact time in CP experiments was monitored in order to obtain values of the cross-polarization time constant (T_{CP}) and $T_{1\rho H}$. In the SPE technique, the ^{13}C signal is generated by nutation of the ^{13}C equilibrium magnetization into the transverse plane by a pulse at the ^{13}C resonance frequency, and the technique therefore does not discriminate between species of different mobility provided the pulse interval is long enough for all nuclei to relax completely. The MAS probe used here contained a large amount of Kel-F fluorinated polymer in the stator housing, which gave a large background signal, ca. 50 kHz wide, in SPE spectra. This background was removed by acquiring the SPE spectrum as a spin−echo[15] using the sequence $\pi/2-\tau-\pi-\tau-$acquire, with the interval τ set to one rotation period.

Results and Discussion

^{1}H Wide-Line Spectra. Figure 1 shows ^{1}H wide-line spectra as a function of exposure time, together with spectra of the CPP and SA monomers for comparison.

The line shape of the polymer showed evidence of a number of components of different line widths arising from regions of different mobility, the proportion of the broadest component increasing with exposure time. The spectra at up to and including 18 h of exposure time were decomposed into three components, designated broad, intermediate, and narrow, while the spectra at longer exposure times were decomposed into two components, designated broad and intermediate. A Gaussian line shape was used for the broad component, and a Lorentzian line shape for the intermediate and narrow components. An example of the three-component decomposition is shown in Figure 2, the line widths and proportions of each component are given in Table 1.

The line widths of the broad and intermediate components remained reasonably constant during degradation. Not unexpectedly, the proportions of broad and intermediate components in the present uneroded poly-

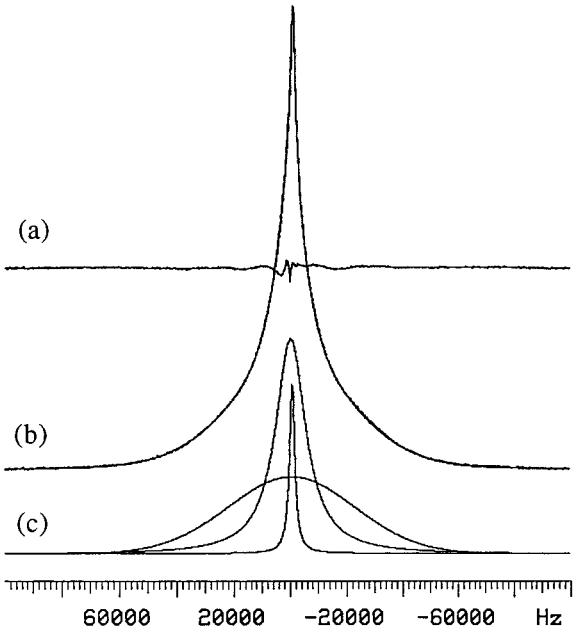

Figure 2. Component analysis of the ^{1}H wide-line spectrum of the original p(CPP:SA) 20:80: (a) the difference between the experimental and simulated spectra; (b) superposed experimental and simulated spectra; (c) the individual broad, intermediate, and narrow components.

mer with 20 mol % CPP lay between those in p(CPP:SA) samples with 12.5 and 30 mol % CPP.[10] The proportion of the broad component increased rapidly even at exposure times as short as 3 h, whereas the narrow component decreased rapidly and was absent after 18 h exposure. This behavior is in marked contrast to that of p(CPP:SA) eroded by phosphate buffer[10] where an intense narrow component (line width ≈1 kHz, intensity fraction ≈60% after 48 h) developed after 12 h of erosion as a result of absorption of up to ca. 70 wt % water. The ^{13}C MAS spectra (see below) showed that degradation proceeds by hydrolysis of the anhydride links and that the rate of hydrolysis by water vapor was essentially the same as that by aqueous buffer. The absence of a narrow component from absorbed water in the eroded polymer in the present work may be explained in terms of a significantly lower rate of absorption from the vapor phase compared to that from the aqueous phase, combined with a comparable rate of hydrolysis after the water has penetrated the polymer. Thus there is no buildup of unreacted mobile water during absorption from the vapor.

The spectra of both monomers were broad, that of SA being somewhat broader than that of CPP. There was no evidence of any significant narrow component from absorbed water. The line width of the broad polymer component fell between those of the monomers. It is likely that the polymer intermediate component arises from amorphous domains formed from chain fragments containing both CPP and SA residues, and the broad component from crystalline domains formed from uniform sequences of several SA units.

Although the broadening of the ^{1}H spectra clearly indicates that the chain mobility is increasingly restricted as degradation proceeds, the origin of this restriction is not clear. Unfortunately, it was not possible to determine whether the carboxylic acid groups detected by the ^{13}C spectra arose from free monomer or chain ends. If the acid groups occur in free monomer, the broadening could arise from the presence of crystalline monomer domains. However, as described below in the section on ^{13}C NMR, the extent of chemical degradation up to 10 h exposure only amounted to ca. 10%, so the initial increase in the broad ^{1}H component proportion from 52% to 83% after 10 h cannot be explained entirely on the basis of an additional contribution from hydrolyzed monomeric residues. More probable explanations for the broadening are (i) the chain mobility is restricted by hydrogen bonding involving the COOH groups and/or (ii) the increase in molecular size resulting from converting an anhydride link into two COOH groups reduces the free volume.

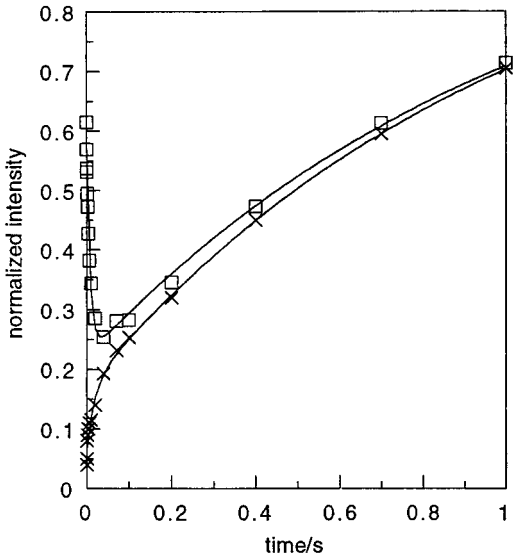

Figure 3. Goldman−Shen ^{1}H spin-diffusion experiment for the original p(CPP:SA) 20:80. The plots show the normalized integrals I_t/I_0 of the broad (×) and narrow (□) components as a function of spin diffusion time t.

For analysis of the T_{1H} and $T_{1\rho H}$ experiments, the polymer line shape was treated simply as having "broad" and "narrow" components, the "narrow" component being defined as the portion of the line lying within the central 10 kHz region (0, 3, 10, and 18 h of exposure) or 20 kHz region (42 and 104 h of exposure), the intensities of these components being determined by integration. Although this division is somewhat arbitrary, any differences in NMR characteristics of the two components can be used as an indicator of the scale of domain heterogeneity. It was found that for each sample the two components had essentially the same value of T_{1H}, indicating that the domains were sufficiently small (on the order of 10 nm or less[16]) to allow averaging of T_{1H} by spin diffusion. The existence of rapid spin diffusion was also revealed by Goldman−Shen experiments, an example of which is shown in Figure 3, which shows plots of the broad and narrow component integrals S_t normalized to their thermal equilibrium integrals S_0 as a function of spin-diffusion time t for the original polymer.

The normalized intensities showed the characteristic properties of rapid spin diffusion; i.e., initially, the narrow component rapidly decreased and the broad component increased until the intensities reached a common value after a diffusion time of ca. 20 ms, and thereafter, the intensities returned to thermal equilibrium at the same rate.

In contrast to T_{1H}, the $T_{1\rho H}$ relaxation curves for each component relaxed at different rates, and moreover, were not a single exponential. Each was analyzed using

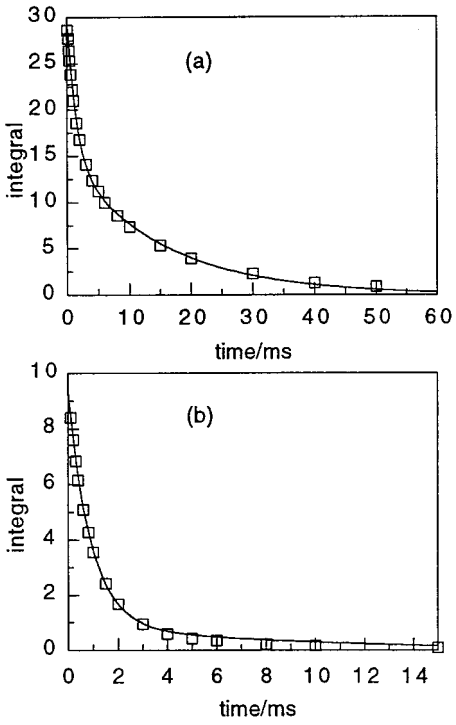

Figure 4. Biexponential fits of the $T_{1\rho}$ decay curves for the original p(CPP:SA) 20:80: (a) broad component; (b) narrow component.

Table 2. Values of ^{1}H T_1 and $T_{1\rho}$ from ^{1}H Relaxation Experiments

		$T_{1\rho}$[b]					
		"broad"[c]			"narrow"[c]		
exposure time/h	T_1/s[a]	fast/ms	slow/ms	% fast	fast/ms	slow/ms	% fast
0	0.96	1.5	16	51	0.85	4.3	85
3	1.43	2.3	20	40	1.0	8.0	76
10	1.45	1.7	19	39	0.94	8.1	79
18	1.45	4.0	28	46	1.3	13	79
42	1.87	3.0	24	32	1.1	12	58
104	2.27	4.3	26	32	1.1	15	47
CPP	3.8	8.2	103	23			
SA	34.3	0.5	290	11			

[a] Estimated uncertainty ±5%. [b] Estimated uncertainty ±10%. [c] See text for definitions of "broad" and "narrow" components.

a biexponential function with fast and slow components, an example fit being shown in Figure 4. The T_{1H} and $T_{1\rho H}$ results are presented in Table 2.

T_1 and $T_{1\rho}$ of the original polymer were considerably shorter than those of either CPP or SA monomer, presumably because of the effect of the relatively mobile amorphous domain. Both T_{1H} and $T_{1\rho H}$ showed a general increase with exposure, presumably due to the formation of more rigid species during the degradation.

^{13}C MAS Spectra. Figure 5 shows the CP/MAS spectra of the original polymer and after erosion for 104 h. Relevant structural units are shown in Chart 1.

The labeled assignments were established with the aid of nonquaternary suppression experiments[17] (which distinguish protonated and nonprotonated carbon atoms), a chemical shift prediction program, and comparison with the spectra of the monomers shown in Figure 6.

The assignments were straightforward except for the peak at 164 ppm. This clearly corresponded with carbon D in the CPP monomer, but there remained the possibility that this peak also comprised the CPP anhydride

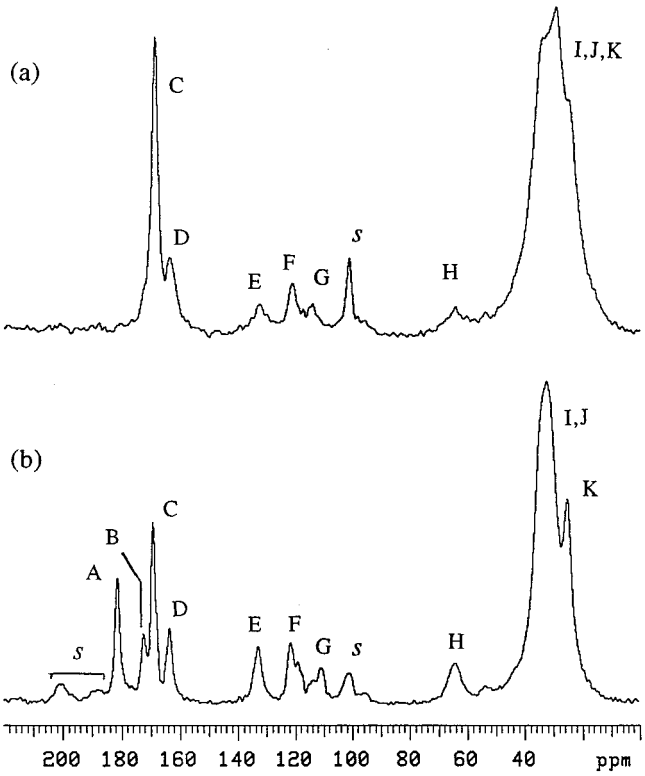

Figure 5. ^{13}C CP/MAS spectrum of (a) the original p(CPP:SA) 20:80 and (b) p(CPP:SA) 20:80 exposed to water vapor for 104 h. The contact time was 1 ms, the recycle time was 5 s, and the spin rate was ca. 5.0 kHz. The label s indicates spinning sidebands from chemical shielding anisotropy (CSA).

Chart 1

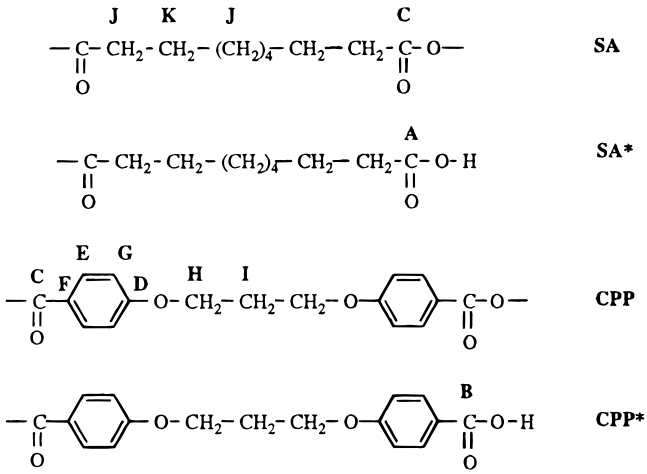

carbonyl carbons, since it might reasonably be expected that the CPP and SA carbonyl carbons would be distinguishable. However, careful measurements allowing for the overlap with peak C showed that its intensity corresponded to the CPP E, F, and G carbons and that its relative intensity remained constant during degradation. It was therefore assigned to CPP carbon D only. Peak C at 169 ppm was assigned to both CPP and SA anhydride carbonyl carbons.

In the spectrum of the sample degraded for 104 h (Figure 5b), there were significant changes in the carbonyl (160−185 ppm) and aromatic (110−140 ppm) regions, and minor changes in the CH_2 region (10−70 ppm). For the present study, the most useful region was the carbonyl region at 160−185 ppm; Figure 7 compares expansions of this region as a function of exposure time.

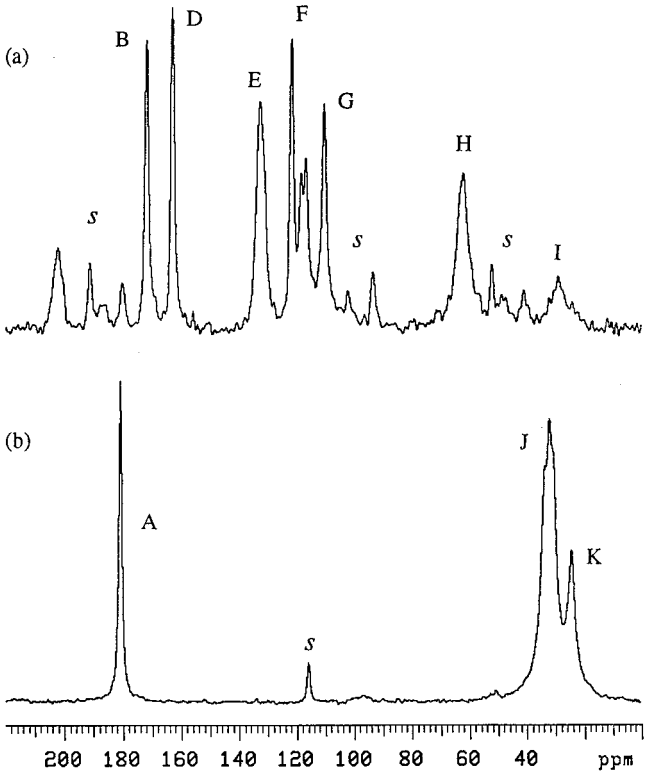

Figure 6. ^{13}C CP/MAS spectra of (a) CPP monomer and (b) SA monomer. Experimental conditions as for Figure 5.

Degradation resulted in a decrease of the polymer anhydride peak at 169 ppm and the appearance of new peaks at 172 and 181 ppm. By comparison with CP/MAS spectra of the monomers, these were assigned to the C=O carbons in carboxylic acid groups of CPP and SA, respectively, designated CPP* and SA* (Chart 1). These peaks directly revealed that degradation occurred by anhydride hydrolysis. Their relative intensity may be used to determine the degree of hydrolysis.

Comparison of the aromatic region revealed some interesting features (Figure 8).

In the CPP monomer spectrum, the resonance of carbon D was split into a doublet, one component of which showed a further doublet splitting. This splitting is almost certainly due to conformational rigidity creating nonequivalence of the two D carbons. Peak G showed no obvious splitting, though it was significantly broader than peak D. In the original polymer, peak D was rather broad and was located at a chemical shift approximately equal to the mean of the D shifts in the monomer, indicating averaging by conformational flexibility. In the polymer degraded for 104 h, peaks for carbon D were observed at shifts corresponding to both polymer and monomer, indicating that the CPP monomer resulting from degradation existed in the same conformation as that of the pure material.

The intensity of peaks in CP spectra depends on contact time t through the equation[18]

$$S_t = \frac{S_0}{\lambda}(1 - e^{-\lambda t/T_{CP}})e^{-t/T_{1\rho H}} \quad (1)$$

where λ is defined by

$$\lambda = 1 - \frac{T_{CP}}{T_{1\rho H}} + \frac{T_{CP}}{T_{1\rho C}} \quad (2)$$

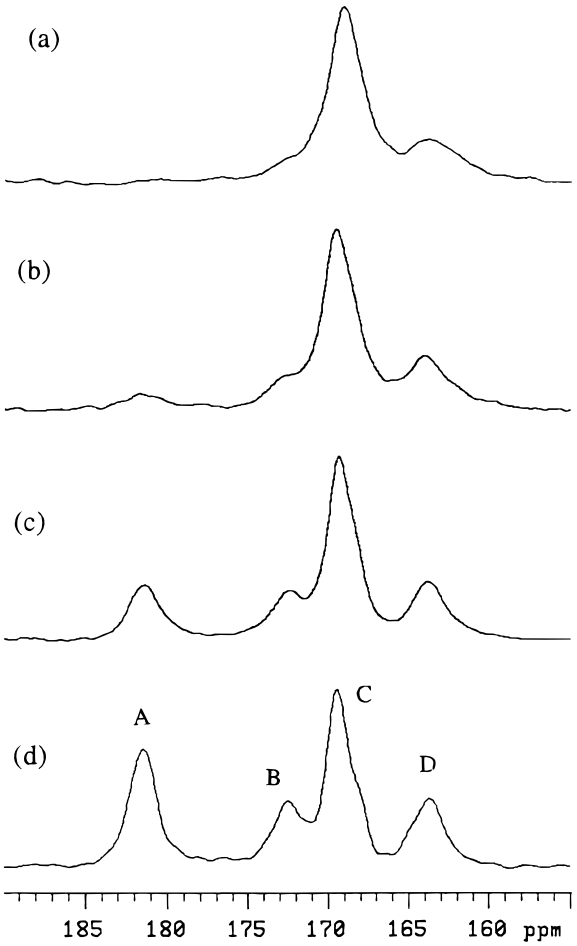

Figure 7. Expansions of the carbonyl region of p(CPP:SA) 20:80 exposed to water vapor: (a) original copolymer; (b) 18 h of exposure; (c) 42 h of exposure; (d) 104 h of exposure. Experimental conditions as for Figure 5 except that the recycle time was 10 s for (c) and 12.5 s for (d).

S_t is the intensity after contact time t, S_0 is the equilibrium CP intensity in the absence of ^1H or ^{13}C rotating frame relaxation, T_{CP} is the time constant for cross-polarization and $T_{1\rho C}$ is the ^{13}C rotating frame relaxation time. T_{CP} depends on the magnitude of the $^1H-^{13}C$ dipolar coupling and the molecular mobility, while $T_{1\rho H}$ depends on the magnitude of the $^1H-^1H$ dipolar coupling and the molecular mobility. T_{CP} and $T_{1\rho H}$ thus depend on the molecular structure and environment, so relative intensities in a single CP spectrum may not be a reliable quantitative measure of the composition. For the present samples, it was found that for the carbonyl peaks, $T_{CP} \approx 0.5$ ms and $T_{1\rho H} \approx T_{1\rho C} \approx 20$ ms. Hence, λ is very close to unity, and eq 1 reduces to

$$S_t = S_0(1 - e^{-t/T_{CP}})e^{-t/T_{1\rho H}} \quad (3)$$

To investigate the impact of differences in T_{CP} and $T_{1\rho H}$, the variation of the ^{13}C intensity as a function of CP contact time was studied. For this purpose, carbonyl peak intensities were obtained as integrals from a line shape component analysis, an example of which is shown in Figure 9. Lorentzian line shapes were assumed for all components. Figure 10 shows the variation of integral with contact time for the carbonyl peaks in the 104 h degraded polymer, together with the least-squares fit according to eq 3.

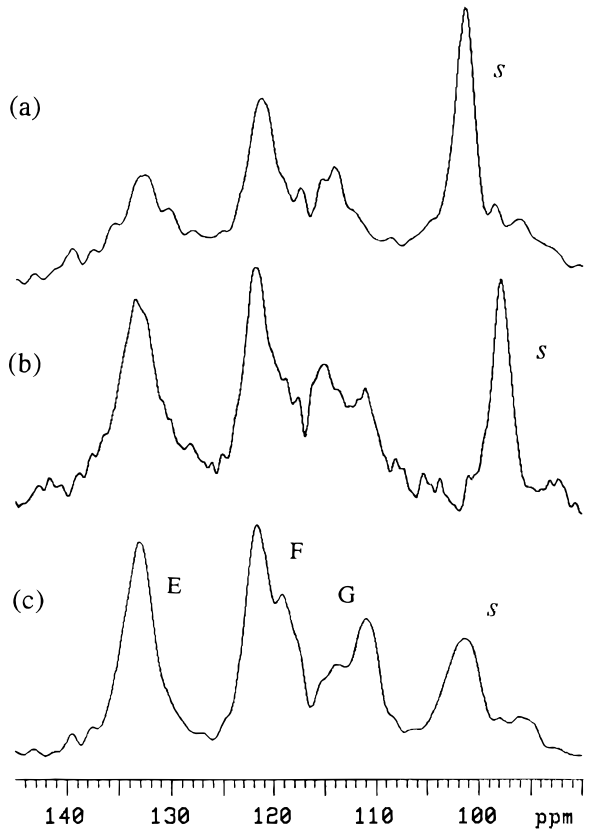

Figure 8. Expansions of the aromatic region of p(CPP:SA) 20:80 exposed to water vapor: (a) original copolymer; (b) 18 h of exposure; (c) 104 h of exposure. Experimental conditions as for Figure 7.

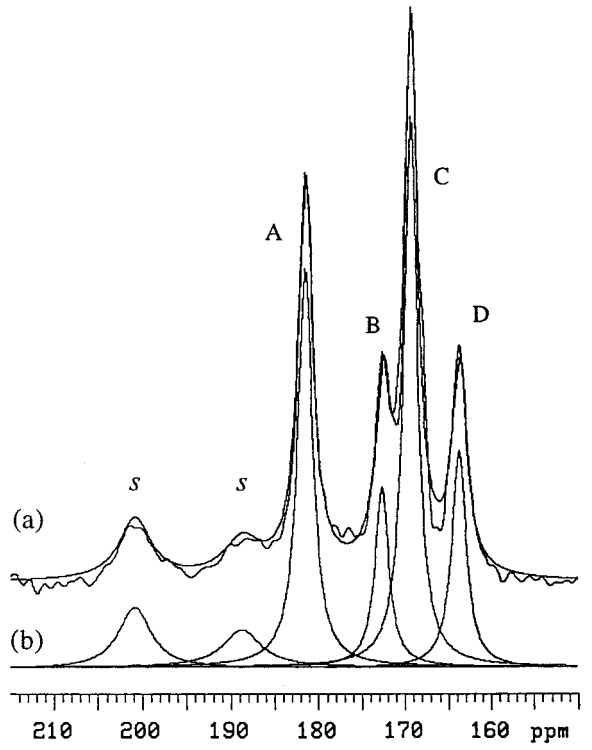

Figure 9. Peak analysis of the carbonyl region of the CP/MAS spectrum of p(CPP:SA) 20:80 exposed for 104 h: (a) superposition of experimental and simulated line shapes; (b) individual components. The contact time was 1 ms, the recycle time was 12.5 s, and the spin rate was 5.0 kHz. The label s indicates CSA spinning sidebands of some aromatic carbons.

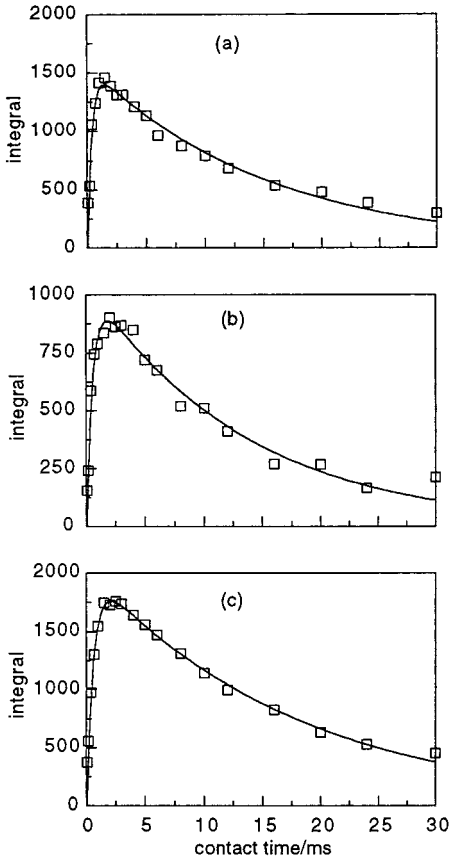

Figure 10. Analysis of the variation with contact time of the integrals of the carbonyl peaks in the CP/MAS spectrum of p(CPP:SA) 20:80 exposed to water vapor for 104 h: (a) SA*; (b) CPP*; (c) SA + CPP anhydride. The recycle time was 12.5 s, and the spin rate was 5.0 kHz.

Table 3. Values of T_{CP} and $T_{1\rho}$ (Both ms) from Variable Contact Time ^{13}C CP/MAS Experiments[a]

	peak							
	SA COOH		CPP COOH		CPP + SA COOOC		CPP C_4	
exposure time/h	T_{CP}	$T_{1\rho}$	T_{CP}	$T_{1\rho}$	T_{CP}	$T_{1\rho}$	T_{CP}	$T_{1\rho}$
0					0.54	11	0.42	7.2
3					0.49	12	0.40	7.6
10					0.61	7.7	0.67	6.6
18	0.44	8.1	0.65	9.5	0.62	8.0	0.69	8.9
42	0.32	13	0.41	14	0.51	15	0.45	12
104	0.37	19	0.57	16	0.63	19	0.56	15
CPP			0.48	64			0.50	57
SA	0.27	52						

[a] Estimated uncertainties are ca. 10%.

This equation represented the integrals within the experimental accuracy. The best-fit values of T_{CP} and $T_{1\rho H}$ are given in Table 3. T_{CP} varied relatively little with structure or exposure time, though the values for the SA carboxylic acid peak at 184 ppm after 42 and 104 h exposure were somewhat shorter than the remaining values, consistent with the relatively short value of T_{CP} in the SA monomer. The values of $T_{1\rho H}$ from ^{13}C NMR were intermediate between the fast and slow values from ^{1}H NMR, due to the fact that the ^{13}C analysis assumed exponential ^{1}H rotating frame relaxation. $T_{1\rho H}$ showed an increase with exposure, consistent with the increase noted above from the direct measurements using ^{1}H spectroscopy.

The composition, expressed as the fraction of carbonyl carbons in SA* and CPP* groups, was determined from the values of S_0 (where reliable) from the variable

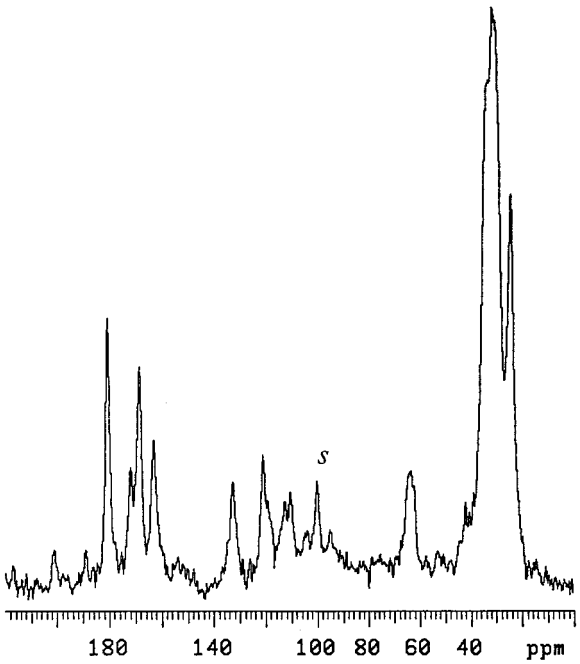

Figure 11. SPE-echo MAS spectrum of p(CPP:SA) 20:80 exposed for 104 h. The recycle time was 100 s, and the spin rate was 5.1 kHz. The label s indicates CSA spinning sidebands.

contact time analyses. Only centerband integrals were used, but examination of the carbonyl first-order high-frequency sidebands showed that the relative intensities of the sidebands were the same as those of the centerbands within experimental error. To check the reliability of the intensities from CP/MAS contact time analysis, the spectrum of the sample exposed for 104 h was also obtained using the SPE-echo technique: see Figure 11.

It was found that a recycle time of 100 s was necessary to ensure full relaxation of all carbons, a time-consuming experiment. The SPE spectrum is similar to the CP/MAS spectrum, though the relative intensities of the peaks are somewhat different because of the effects of T_{CP} and $T_{1\rho H}$ in the CP spectra. The carbonyl integrals in the SPE spectrum give fractions of 0.33 and 0.22 for SA* and CPP*, respectively, in excellent agreement with the corresponding values of 0.34 and 0.23 from the CP experiments.

The compositions from the present work are shown in Figure 12, together with, for comparison, the same fractions obtained previously[10] for the erosion of p(CPP:SA) 12.5:87.5 by aqueous buffer at 37 °C; in that work, the copolymer was in the form of pressed disks of diameter 10.4 mm and thickness 1.1 mm.

It is evident that the rates of anhydride hydrolysis in the two polymers are comparable despite the difference in the erosion conditions. The facts that SA* for p(CPP:SA) 12.5:87.5 is greater than for p(CPP:SA) 20:80 and CPP* for p(CPP:SA) 12.5:87.5 is less than for p(CPP:SA) 20:80 are attributable to the greater proportion of SA in p(CPP:SA) 20:80. In both cases, the proportion of SA* units was significantly greater than the proportion of CPP* units, indicating comparable hydrolysis rates of SA−SA and SA−CPP anhydride links. The decrease in SA* for p(CPP:SA) 12.5:87.5 after an erosion time of 40 h may be attributed to dissolution of the SA monomer in the aqueous buffer.

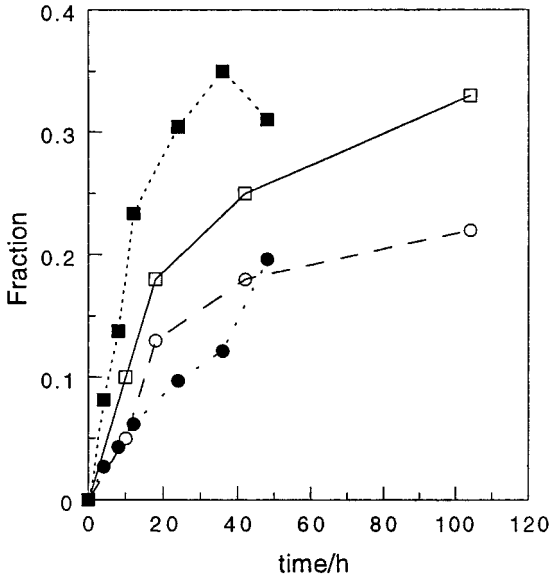

Figure 12. Fractions of carboxylic acid groups in eroded p(CPP:SA): (□) SA* in p(CPP:SA) 20:80 eroded by water vapor; (○) CPP* in p(CPP:SA) 20:80 eroded by water vapor; (■) SA* in p(CPP:SA) 12.5:87.5 eroded by aqueous buffer; (●) CPP* in p(CPP:SA) 12.5:87.5 eroded by aqueous buffer. p(CPP:SA) 12.5:87.5 data from ref 10.

Acknowledgment. This work was supported by grants from the Royal Society to R.V.L. and from the EPSRC toward the purchase of the NMR spectrometer. The authors thank Mohamad Erfan for the synthesis of the polymer.

References and Notes

(1) Mathiowitz, E.; Jacob, J.; Pekarek, K.; Chickering, D. *Macromolecules* **1993**, *26*, 6, 6756.
(2) Tamada, J. A.; Langer, R. *Proc. Natl. Acad. Sci. U.S.A.* **1993**, *90*, 552.
(3) Shakesheff, K. M.; Davies, M. C.; Domb, A.; Jackson, D. E.; Roberts, C. J.; Tendler, S. J. B.; Williams, P. M. *Macromolecules* **1995**, *28*, 8, 1108.
(4) Mäder, K.; Bacic, G.; Domb, A.; Elmalak, O.; Langer, R.; Swartz, H. M. *J. Pharm. Sci.* **1997**, *86*, 126.
(5) Mäder, K.; Nitschke, S.; Stosser, R.; Borchert, H.-H.; Domb, A. *Polymer* **1997**, *38*, 4785.
(6) Göpferich, A.; Langer, R. *J. Polym. Sci., Part A: Polym. Chem.* **1993**, *31*, 2445.
(7) Göpferich, A. *Biomaterials* **1996**, *17*, 103.
(8) Ron, E.; Mathiowitz, E.; Mathiowitz, G.; Domb, A.; Langer, R. *Macromolecules* **1991**, *24*, 2278.
(9) Mathiowitz, E.; Kreitz, M.; Pekarek, K. *Macromolecules* **1993**, *26*, 6749.
(10) McCann, D. L.; Heatley, F.; D'Emanuele, A. *Polymer*, submitted.
(11) Domb, A. J.; Langer, R. *J. Polym. Sci., Part A: Polym. Chem.* **1987**, *25*, 3373.
(12) McBrierty, V. J.; Packer, K. J. *Nuclear Magnetic Resonance in Solid Polymers*; Cambridge University Press: Cambridge, U.K., 1993; Chapter 2.
(13) Goldman, M.; Shen, L. *Phys. Rev.* **1966**, *144*, 321.
(14) Reference 9, pp 102ff.
(15) Reference 9, p 93.
(16) Reference 9, p 196.
(17) Reference 9, pp 106−108.
(18) Reference 9, p 47.

MA971652J